

Original Paper

# Retracted: Treatment of Left Ventricular Circulation Disorder: Application of Echocardiography Information Data Monitoring

Yulong Chen<sup>1</sup>, MD; Jianxia Du<sup>1</sup>, BD; Xiao Sun<sup>1</sup>, BD; Qiancheng Li<sup>1</sup>, BD; Ming Qin<sup>1</sup>, MD; Qian Xiao<sup>2</sup>, BD; Mark Bryan<sup>3</sup>, PhD

<sup>1</sup>Department of Ultrasound, Xuzhou Children's Hospital, Xuzhou Medical University, Xuzhou, China

<sup>2</sup>Department of Emergency, Xuzhou Central Hospital, Xuzhou, China

<sup>3</sup>Dipartimento di Biomedicina, Università di Torino, Torino, Italy

**Corresponding Author:**

Qian Xiao, BD

Department of Emergency

Xuzhou Central Hospital

199 Jiefang South Road, Quanshan District

Xuzhou, 221000

China

Phone: 86 0516 83956400

Email: [xiaoqianleo968@163.com](mailto:xiaoqianleo968@163.com)

**Related Article:**

Do not cite this article - this article has been retracted. Retraction notice: <https://medinform.jmir.org/2026/1/e98672>

## Abstract

**Background:** Cardiac hypertrophy induced by pressure overload is one of the important causes of heart failure and sudden cardiac death. At present, there are few studies on the outcome of left ventricular hypertrophy and left ventricular function after complete pressure load removal.

**Objective:** This study aims to better simulate the changes of left ventricular structure and function during the process of left ventricular pressure overload and unloading, and to explore the application of echocardiography in it.

**Methods:** In this study, healthy male (BALB/C) mice were used as research objects to establish an ascending aorta constriction model, to carry out echocardiographic and hemodynamic examinations, to establish an ascending aorta deconstriction model in mice, and to carry out echocardiographic and hemodynamic examinations.

**Results:** Compared with the sham operation group, the left ventricular end-systolic diameter (LVESD), left ventricular end-diastolic diameter (LVEDD), interventricular septal (IVS), and left ventricular posterior wall (LVPW) in the constriction operation group were significantly increased ( $P=.02$ ,  $P=.02$ ,  $P=.02$ , and  $P=.02$ , respectively). LVESD, LVEDD, IVS, and LVPW in the early and late constriction groups were significantly decreased, and the degree of decrease in the early group was greater than that in the late group; compared with the sham operation group, left ventricular diastolic pressure in the constriction operation group increased significantly at 9 and 15 weeks after operation ( $P=.03$ ). Left ventricular systolic pressure at 15 weeks after operation decreased to a certain extent but was higher than that of the sham operation group ( $P=.02$ ). The maximal rate of the increase of left ventricular pressure at 3 weeks, 9 weeks, and 15 weeks after operation decreased significantly ( $P=.03$ ,  $P=.02$ , and  $P=.02$ , respectively).

**Conclusions:** In this study, the ascending aorta coarctation model and descending aorta coarctation model were successfully established, which verifies the value of echocardiography information data monitoring in the treatment of left ventricular circulation disorders and the evaluation of surgical treatment.

(*JMIR Med Inform* 2020;8(9):e19110) doi: [10.2196/19110](https://doi.org/10.2196/19110)

**KEYWORDS**

echocardiography information; data monitoring; hemodynamics; left ventricular circulation disorder

## Introduction

The diastolic process of the heart is an important part of the cardiac cycle. If abnormal physiological function occurs in this part, it will lead to left ventricular diastolic dysfunction, which will lead to the decline of left ventricular compliance and relaxation, leading to heart disease. Hypertension and aortic stenosis account for a large proportion of adult heart disease in China. Their common characteristics are that they lead to left ventricular pressure overload and then left ventricular hypertrophy [1,2]. Usually, surgical replacement of the stenosed aortic valve and control of blood pressure can reverse left ventricular hypertrophy and improve the survival rate of patients. However, the recovery of cardiac function in some patients with aortic stenosis after operation is not ideal [3]. In addition, some surveys show that about 15%-20% of patients with hypertension without left ventricular hypertrophy will develop left ventricular hypertrophy during treatment [4]. Although patients with left ventricular hypertrophy receive adequate antihypertensive treatment, the incidence of cardiovascular adverse events is still higher than those without left ventricular hypertrophy [5]. Therefore, it is inappropriate to treat left ventricular hypertrophy inhibitors only. At present, most of the literature about left ventricular hypertrophy focuses on its pathogenesis, molecular mechanism, and the changes of left ventricular function after intervention with pressure overload [6,7]. However, there are few studies on the outcome of left ventricular hypertrophy and left ventricular function after complete removal of pressure load. The evaluation of left ventricular function is the most important index in the diagnosis of various cardiovascular diseases and the evaluation of drug treatment effect. It can predict whether patients have heart failure, and it plays an important role in the clinic [8]. Therefore, it is necessary to establish an ideal left ventricular hypertrophy model and its reversal model, and to explore the characteristics of left ventricular structure and function during the process of left ventricular pressure overload-unloading through effective diagnostic means.

Studies have shown that echocardiography can evaluate the characteristics of left ventricular thickness, left ventricular volume, and wall motion, and it is a widely used auxiliary examination method for judging left ventricular diastolic function in the clinic [9]. The heart rate of mice is generally between 300-500 BPM, and the ventricular cavity is small, so ordinary echocardiography cannot obtain a clear image [10]. In recent years, as the ultrasound technology develops, especially the appearance of high-frequency probes, the reliability of mouse heart function ultrasound evaluation has been improved. Wang et al [11] explored the evaluation value of echocardiography in the structure and function of the mouse myocardial infarction model. In addition, they believed that echocardiography can accurately and sensitively detect the location and severity of myocardial infarction, providing an important basis for clinical diagnosis and treatment of myocardial infarction [11]. It can be seen that echocardiography has a broad application prospect in the evaluation of mouse heart function. In this study, the whole heart function of the animal model is evaluated by

echocardiography, and the left ventricular blood circulation is evaluated.

In summary, to establish ascending aorta constriction animal models and ascending aorta deconstriction animal models, and to verify the application value of echocardiography in evaluating the whole heart function of animal models, mice were taken as the research objects to explore the application of echocardiography in the diagnosis and treatment of left ventricular blood circulation disorders in mice so as to provide a basis for left ventricular hypertrophy. Reversal research provides an excellent animal model and provides a reference for the monitoring of coronary heart disease and heart failure.

## Methods

### Experimental Animal and Groups

A total of 60 healthy male BALB/c mice (XXX Animal Center) aged 6-8 weeks and weighing about 18-25 g were selected as experimental subjects. All animals were fed in cages with national standard rodent feed, with 4 in each cage. Mice could eat and drink freely. There was no significant difference in body weight between groups. The feeding environment had natural light. The room temperature was controlled at 20-26 °C, and the humidity was controlled at 40%-50%. The mice were fed adaptively for 2 weeks. Animal handling and experimental procedures conformed to the National Laboratory Animal standards and were approved by the ethical committee.

All mice were randomly divided into 6 groups, 10 in each group, namely, sham operation group, 3-week constriction operation group, 9-week constriction operation group, 15-week constriction operation group, early deconstriction group, and late deconstriction group.

### Establishment of Ascending Aorta Coarctation Model in Mice

In addition to sham-operated mice, other mice were intraperitoneally injected with 2% tribromethanol at a dose of 25 mg/kg (Shanghai Jingke Chemical Technology Co, Ltd, China). After successful anesthesia, the mice were fixed in supine position on the operating table (Beijing Semiconductor Equipment Factory, China). During the operation, if the depth of anesthesia was not enough, 2% tribromethanol could be added, but the anesthesia could not be too deep. Hair was cut off from the neck and upper chest of mice, and iodophor (Beijing Baioubowei Biotechnology Co, Ltd., China) was used to disinfect them. Plastic tubes suitable for size were inserted into the trachea through the mouth and connected to a small animal ventilator (Shenzhen Reward Life Technology Co, Ltd, China) to assist mice in breathing. The skin was cut from the upper sternum to the medial side of the external jugular vein, and the subcutaneous fascia was separated to expose the superficial muscles of the neck. The muscles were cut and divided into two sides along the median line to expose the trachea. In mice, the thymus was pulled apart, and the surrounding tissues of ascending aorta were separated so that the aortic arch was fully exposed. The aortic arch was separated and the 4-0 Prolene line (Shanghai Yuyan Scientific Instruments Co, Ltd, China) was used to circumvent and tie the aortic arch. We were careful not

to ligate and leave space for gaskets and needles. The 27G needle was placed in the para-aortic junction, and then the gasket was inserted to tighten the junction rapidly. After ligation, needles needed to be removed quickly. Ligation should be done accurately and quickly, keeping in situ as far as possible to prevent damage to the ascending aortic adventitia. After ligation, penicillin (100,000 units, Shijiazhuang Best Pharmaceutical and Chemical Co, Ltd, China) should be sprayed into the chest cavity. The thymus glands were seamless, the thoracic glands were closed layer by layer, and the skin was sutured. In the sham operation group, the ascending aorta was separated without ligation, and the other procedures were the same.

### **Echocardiographic Examination of Ascending Aorta Coarctation in Mice**

Echocardiography was performed in mice before and 3, 9, and 15 weeks after ascending aortic coarctation. Fasting was required 4-6 hours before the examination. The mice were given intraperitoneal injection of 2% tribromethanol at a dose of 15 mg/kg and fixed on the examination table in supine position to remove the hair on the chest, upper abdomen, and the roots of both upper limbs. First, a sodium sulfide solution (8%, Shanxi Xinchengshun Chemical Co, Ltd, China) was used to rinse and depilate. Clean water was then used for flushing. Attention was paid to check whether the area's hair was completely removed. The VIVID7 Echocardiograph Diagnostic Instrument (GE Company, United States) was used for echocardiographic examination in mice. The probe frequency was 12 MHz, and the observation sites were bilateral thoracic cavity and subxiphoid process of mice. The indicators included left ventricular end-systolic diameter (LVESD), left ventricular end-diastolic diameter (LVEDD), interventricular septal (IVS), and left ventricular posterior wall (LVPW).

### **Hemodynamic Study of Ascending Aorta Coarctation in Mice**

The mice were intraperitoneally injected with 2% tribromethanol at a dose of 25 mg/kg and fixed on the operating table in supine position. Hair was cut off from the neck and upper chest. Sodium sulfide ethanol solution was used to rinse and depilate hair and then disinfected with iodophor. The aseptic cave towel was laid, and a longitudinal incision about 2 cm long was made along the middle of the neck. Skin and subcutaneous fascia were cut to expose neck muscles. The sternohyoid muscles were bluntly separated from each other to expose the trachea. The right muscular layer was sutured and fixed on the operating table by a needle with thread No 0. In the groove of the trachea and right sternohyoid muscle, the internal carotid artery was found and separated, and two silk threads were pierced. The distal end of the right internal carotid artery was ligated and slightly pulled outward by the filament near the central end. The Pre-Chong Heparin (Shanghai Kanglang Biotechnology Co, Ltd, China) No 24 intravenous indwelling needle (Anhui Hongzhong Medical Devices Co, Ltd, China) was used to puncture arteries. After the puncture, the needle core was extracted and connected with the preflushed heparin pressure transducer (Beijing Zhishu Duobao Biotechnology Co, Ltd, China). Internal carotid artery pressure was observed on a multifunctional physiological recorder (ML870, Powerlab, Australia). The silk thread was

released, and we inserted a venous indwelling needle into the heart. During the operation, attention was paid to the change of pressure on the display. If the pressure suddenly increased, it indicated that it had entered the left ventricle. Silk thread was used to tie a knot outside the blood vessel and fix the intravenous indwelling needle to prevent blood leakage. However, it should be noted that knotting should not be too tight. Once the connection was successful and the waveform was stable, it was necessary to start recording data, including left ventricular diastolic pressure (LVDP), left ventricular systolic pressure (LVSP), maximal rate of the increase of left ventricular pressure (+dp/dt Max), and maximal rate of the decrease of left ventricular pressure (-dp/dt Max).

### **Establishment of Ascending Aorta Deconstriction Mouse Model**

At 3 and 9 weeks after ascending aorta coarctation, ascending aorta coarctation was performed on mice in the early and late decoarctation groups. The mice were intraperitoneally injected with 2% tribromethanol at a dose of 25 mg/kg and fixed on the operating table in supine position. The hair was cut off from the neck and upper chest. It was necessary to rinse and depilate with sodium sulfide ethanol solution and then disinfect with iodophor. Small animal ventilators were connected to assist mice in breathing, exposing the trachea. The thoracotomy was performed between the two or three ribs, and the thymus was opened to expose the aortic arch. The original ligation line was found. Down the ligation line, the gasket was separated. Penicillin (100,000 units) was sprayed in the chest cavity. The thymus was not seamed. It was then necessary to close the chest layer by layer and suture the skin.

### **Echocardiographic Examination of Ascending Aorta Decoarctation Model in Mice**

Echocardiography was performed in mice at 3, 9, and 15 weeks after deconstriction. The mice were intraperitoneally injected with 2% tribromethanol at a dose of 15 mg/kg and fixed on the examination table in supine position. Hair was removed from the chest, upper abdomen, and the roots of both upper limbs. It was necessary to rinse with sodium sulfide solution and then rinse with water. The VIVID7 echocardiographic diagnostic instrument was used to perform echocardiographic examination in mice. Detection indicators included LVESD, LVEDD, IVS, and LVPW.

### **Hemodynamic Study of Ascending Aorta Decoarctation in Mice**

The mice were intraperitoneally injected with 2% tribromethanol at a dose of 25 mg/kg and fixed on the operating table in supine position. Hair was cut off from the neck and upper chest. It was first necessary to rinse and depilate with sodium sulfide ethanol solution and then disinfect with iodophor. The aseptic cave towel was laid. Along the middle of the neck, an incision about 2 cm in length was made to expose the trachea. A No 0 thread was used to suture and fix the right muscular layer on the operating table. In the groove of the trachea and right sternohyoid muscle, the internal carotid artery was found and separated, and two silk threads were pierced. The distal end of the right internal carotid artery was ligated and slightly pulled

outward by the filament near the central end. A preflushed heparin 24 venous indwelling needle was used to puncture the artery. After the puncture was completed, the needle core needed to be pulled out and connected with the pressure transducer for preflushing heparin. The internal carotid artery pressure was observed on a multifunctional physiological recorder. To loosen the silk thread, a venous indwelling needle was inserted into the heart. During the operation, it was necessary to pay attention to the pressure changes on the display. If the pressure suddenly increased, it indicated that it had entered the left ventricle. Silk thread was used to tie a knot outside the blood vessel to fix the intravenous indwelling needle to prevent blood leakage, but it should be noted that the knot should not be too tight. After the connection was successful and the waveform was stabilized, data were recorded, including LVDP, LVSP, +dp/dt max, -dp/dt max.

### Statistical Methods

SPSS 26.0 (IBM Corp) statistical software was used to analyze the data. The measurement data was expressed as mean and standard deviation. The mean of the two samples was compared by the *t* test. The counting data was expressed as incidence *n* (%). The comparison used the chi-square test, and the difference was statistically significant when  $P < .05$ .

## Results

### Echocardiographic Results of Ascending Aorta Coarctation Mouse Model and Ascending Aorta Decoarctation Mouse Model

The results of echocardiography in ascending aorta coarctation mice and ascending aorta decoarctation mice are shown in [Figures 1](#) and [2](#). From the ascending aorta coarctation model in mice, it can be seen that, compared with the sham operation group, the LVESD, LVEDD, IVS, and LVPW of the coarctation operation group increased significantly with statistical significance ( $P = .02$ ,  $P = .02$ ,  $P = .02$ , and  $P = .02$ , respectively). In the constriction group, compared with the preoperative group, LVESD, LVEDD, IVS, and LVPW in mice increased significantly 3 weeks after the operation with statistical significance ( $P = .01$ ,  $P = .01$ ,  $P = .02$ , and  $P = .01$ , respectively), suggesting that the mice had centripetal hypertrophy. Compared with 3 weeks after the operation, the LVESD, LVEDD, and IVS of mice increased significantly at 9 weeks after the operation with statistical significance ( $P = .02$ ,  $P = .01$ , and  $P = .02$ , respectively), while the increase of LVPW was not significant, suggesting that the mice have eccentric hypertrophy ([Figure 2A](#)). Compared with 9 weeks after operation, LVESD and LVEDD in mice increased significantly at 15 weeks after the operation, and the difference was statistically significant ( $P = .03$  and  $P = .03$ , respectively), suggesting that heart failure occurs in mice.

**Figure 1.** Echocardiographic results of ascending aorta coarctation mouse model and ascending aorta decoarctation mouse model (A: LVESD; B: LVEDD; C: IVS; D: LVPW). IVS: interventricular septal; LVEDD: left ventricular end-diastolic diameter; LVESD: left ventricular end-systolic diameter; LVPW: left ventricular posterior wall; W: weeks.

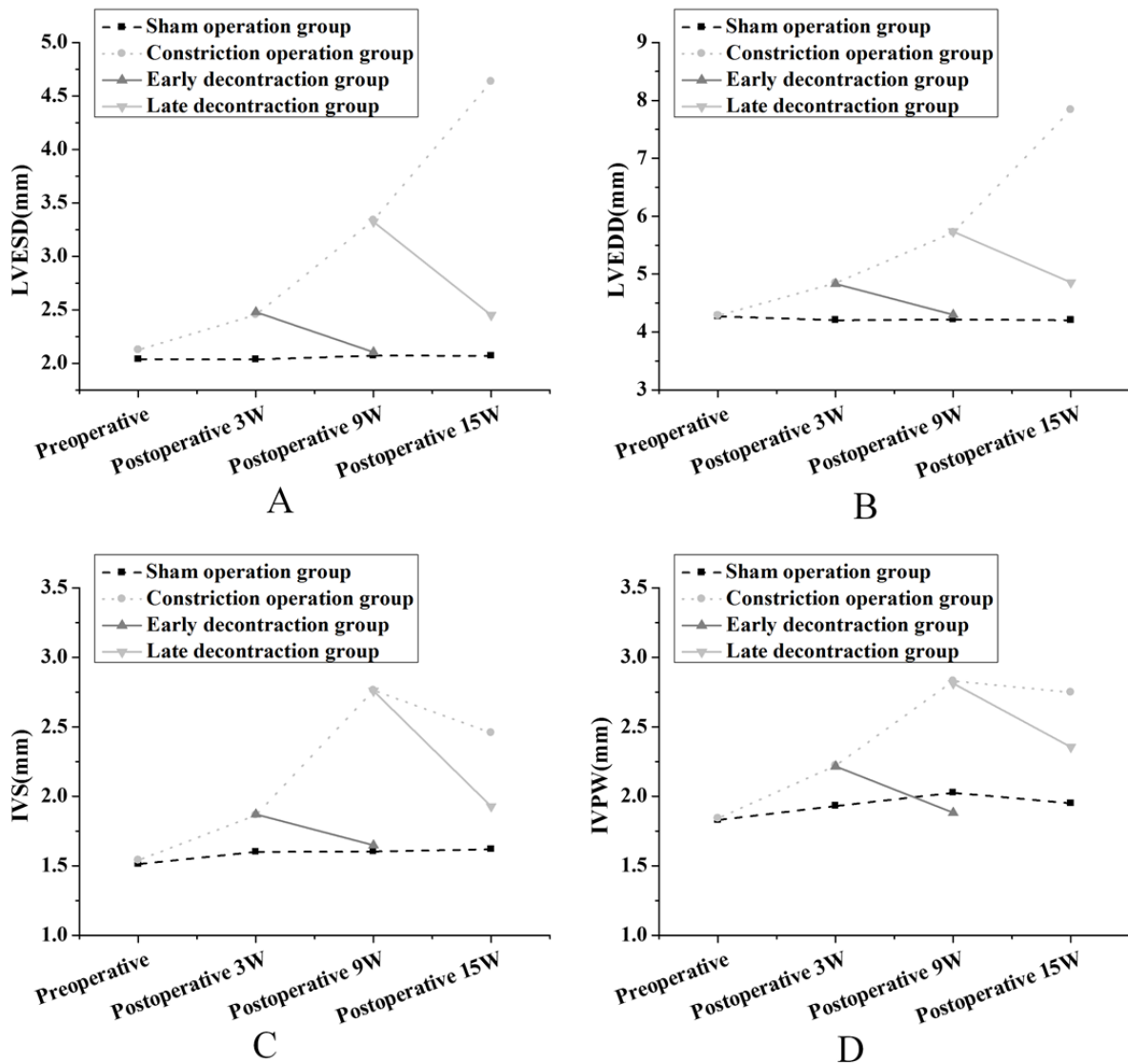
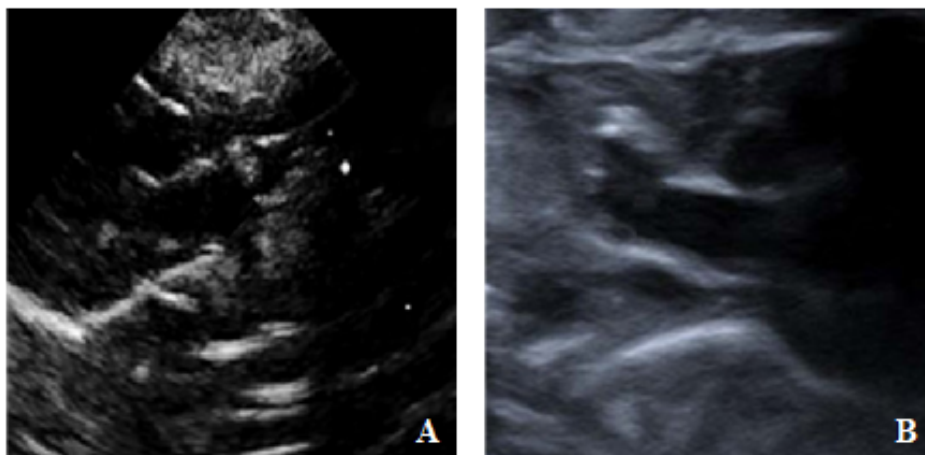


**Figure 2.** Echocardiography of mice (A: ascending aorta constriction mouse model; B: ascending aorta deconstriction mouse model).



From the model of ascending aorta deconstriction mice, it can be seen that, compared with the operation group, the left

ventricular function of the early decontraction group and the late decontraction group were reversed, the blood circulation

disorder was improved, and the effect of the early deconstriction group was more obvious than that of the late deconstriction group. In the early deconstriction group, the LVESD, LVEDD, IVS, and LVPW of mice decreased significantly at the 9th week and tended toward the initial level (Figure 2B). In the delayed deconstriction group, the levels of LVESD, LVEDD, IVS, and LVPW decreased significantly at the 15th week but could not return to the initial level, suggesting the persistence of ventricular hypertrophy and the persistence of left ventricular circulation disorders.

### Hemodynamic Results of Ascending Aorta Coarctation Mice Model and Ascending Aorta Decoarctation Mice Model

The hemodynamic results of the ascending aorta coarctation mice and ascending aorta decoarctation mice are shown in Table

1. From the ascending aorta coarctation model in mice, it can be seen that, compared with the sham operation group, there was no difference in LVDP in the coarctation group 3 weeks after operation. At 9 weeks and 15 weeks after the operation, the LVDP of mice in the constriction group increased significantly ( $P=.03$  and  $P=.03$ , respectively). Compared with the sham-operated group, the LVSP in the constriction group increased significantly at 3 weeks and 9 weeks after the operation ( $P=.03$  and  $P=.02$ , respectively). At 15 weeks after the operation, the LVSP of the constriction group decreased to a certain extent but was higher than that of the sham operation group ( $P=.02$ ). Compared with the sham-operated group, the  $-dp/dt$  max in the constriction group decreased significantly at 3 weeks, 9 weeks, and 15 weeks ( $P=.03$ ,  $P=.02$ , and  $P=.02$ , respectively). The results of hemodynamics were consistent with those of echocardiography.

**Table 1.** Hemodynamic results of ascending aorta constriction model and ascending aorta deconstriction model in mice.

Period	LVDP <sup>a</sup> (mmHg)	LVSP <sup>b</sup> (mmHg)	+dp/dt max <sup>c</sup> (mmHg/sec)	-dp/dt max <sup>d</sup> (mmHg/sec)
Sham operation group	4.8	125	6400	4700
3-week constriction surgery group	4.9	168	5000	3950
9-week constriction surgery group	8.1	175	5200	3500
15-week constriction surgery group	14.8	172	4200	3400
Early deconstriction group	4.9	120	6000	4100
Late deconstriction group	6.3	141	5600	4080

<sup>a</sup>LVDP: left ventricular diastolic pressure.

<sup>b</sup>LVSP: left ventricular systolic pressure.

<sup>c</sup>+dp/dt max: maximal rate of the increase of left ventricular pressure.

<sup>d</sup>-dp/dt max: maximal rate of the decrease of left ventricular pressure.

In the ascending aorta deconstriction mice model, compared with the sham-operated mice, the differences of LVDP, LVSP, and +dp/dt max in the early deconstriction mice were not statistically significant, while -dp/dt max was significantly lower ( $P=.03$ ). Compared with the constriction operation group, the LVDP and LVSP in the early deconstriction group were significantly lower, and the +dp/dt max and -dp/dt max were significantly higher. It was observed that the left ventricular function of ascending aorta deconstriction mice was restored, and the blood circulation disorder had been improved. Compared with the constriction operation group, the LVDP and LVSP of mice in the delayed deconstriction group decreased significantly ( $P=.03$  and  $P=.02$ ), and the +dp/dt max and -dp/dt max increased significantly, with statistical significance ( $P=.03$  and  $P=.04$ , respectively). The results of hemodynamics were consistent with those of echocardiography.

## Discussion

### Result Analysis

In the past, most of the animal models of left ventricular hypertrophy under pressure overload were established by ligation of the abdominal aorta. This model is easy to operate and has a high survival rate, but the modeling time is too long, sometimes even more than 1 year [12]. In recent years, some

scholars have proposed models of aortic arch and ascending aorta coarctation, but the models need the support of endotracheal intubation and artificial ventilation conditions [13]. However, ligation of the aortic arch can increase the pressure of the right brain and its limbs, increase the collateral circulation through the head and arm, and then reduce the afterload, making the modeling a failure [14].

To establish an ideal model of left ventricular hypertrophy and its reversion, and simulate the changes of left ventricular structure and function during the process of left ventricular pressure overload and deload, the healthy male BALB/c mice were taken as the research objects, and the models of ascending aorta constriction mice and ascending aorta deconstriction mice were established. To evaluate the success of the model, echocardiography and hemodynamics were performed. Echocardiography has the advantages of a noninvasive and simple operation, which can reflect the left ventricular function and wall thickness. The heart rate of mice was fast and the ventricular cavity was small, and M-mode ultrasound can make the imaging clearer and provide accurate indexes such as the diameter of the ventricular cavity and the thickness of the ventricular wall.

The results of this study showed that the LVESD, LVEDD, IVS, and LVPW of the mice in the operation group increased significantly compared with those before operation ( $P=.01$ ,

$P=.01$ ,  $P=.02$ , and  $P=.01$ , respectively), suggesting that there was centripetal hypertrophy in the mice. At this time, the increased myocardial contractility can fully compensate for the increase of pressure load. The previously mentioned indexes showed a further upward trend in the 6th and 9th weeks after operation. At the 9th week after operation, the LVESD, LVEDD, and IVS of the mice in the constriction group increased significantly, while the LVPW increased slightly, suggesting that the mice appeared to have centrifugal hypertrophy. At 15 weeks after the operation, the LVESD and LVEDD of the mice in the constriction group increased significantly, indicating that the mice had heart failure. The detection of left ventricular pressure can directly prove the success of the aortic coarctation model and the degree of coarctation. It was found that the left ventricular pressure increased significantly after ascending aortic coarctation, which indicated that the model was constructed successfully. In the early group, IVS and LVPW decreased to nearly the initial level 3 weeks after the removal of systole, and LVESD and LVEDD recovered completely 6 weeks after the removal of systole. There were also differences in left ventricular function between the late group and the early group, suggesting that the reversal of left ventricular hypertrophy was related to the duration.

### Research Reliability

The results of hemodynamics were consistent with those of echocardiography, which further proved the reliability of echocardiography. Hendrikx et al [15] showed that in the mouse model of myocardial infarction, echocardiography could provide

reliable measurement of left ventricular function with high accuracy. It showed that echocardiography had important application value in the evaluation of mouse heart function, which was consistent with the results of this study.

Based on the model of ascending aorta coarctation, the model of ascending aorta decoarctation in mice was established, and the accuracy and reliability of the modeling method were verified. Echocardiography can accurately measure the left ventricular function of mice, which has important application value in the diagnosis of left ventricular blood circulation disorder and the evaluation of surgical treatment effect.

### Conclusion

The application of echocardiography in the diagnosis and treatment of left ventricular blood circulation disorders in mice was explored. Through research, it was found that echocardiography can accurately measure the left ventricular function of mice and has important application value in the diagnosis of left ventricular blood circulation disorders and the evaluation of surgical treatment effect. It provides an excellent animal model for the study of left ventricular hypertrophy and its reversion, and provides a reference for the monitoring of coronary heart disease and heart failure. However, there are some deficiencies in the research process, such as the small number of experimental animals, which leads to a certain degree of deviation in the results. Therefore, in the later research process, the number of experimental animals will be further increased to make the results more valuable for reference.

### Conflicts of Interest

None declared.

### References

1. Wulin G, Guohua D, Tong Z, Dongxue B, Chunhua L, Xiaojing S, et al. Tonifying Qi and activating blood circulation in terms of Traditional Chinese Medicine: their effects in patients with myocardial infarction. *J Tradit Chin Med*. Oct 2018;38(5):726-732. [doi: [10.1016/s0254-6272\(18\)30911-7](https://doi.org/10.1016/s0254-6272(18)30911-7)]
2. Cho I, Chang H, Heo R, Kim I, Sung JM, Chang B, et al. Association of thoracic aorta calcium score with left ventricular hypertrophy and clinical outcomes in patients with severe aortic stenosis after aortic valve replacement. *Ann Thorac Surg*. Jan 2017;103(1):74-81. [doi: [10.1016/j.athoracsur.2016.05.039](https://doi.org/10.1016/j.athoracsur.2016.05.039)] [Medline: [27440307](https://pubmed.ncbi.nlm.nih.gov/27440307/)]
3. Burgos PFM, Luna Filho B, de Assis Costa F, Bombig MTN, de Souza D, Bianco HT, et al. Electrocardiogram performance in the diagnosis of left ventricular hypertrophy in hypertensive patients with left bundle branch block. *Arq Bras Cardiol*. Jan 2017;108(1):47-52. [FREE Full text] [doi: [10.5935/abc.20160187](https://doi.org/10.5935/abc.20160187)] [Medline: [27992034](https://pubmed.ncbi.nlm.nih.gov/27992034/)]
4. El Saiedi SA, Mira MF, Sharaf SA, Al Musaddar MM, El Kaffas RMH, AbdelMassih AF, et al. Left ventricular diastolic dysfunction without left ventricular hypertrophy in obese children and adolescents: a Tissue Doppler Imaging and Cardiac Troponin I Study. *Cardiol Young*. Aug 07, 2017;28(1):76-84. [doi: [10.1017/s1047951117001627](https://doi.org/10.1017/s1047951117001627)]
5. Cariou E, Bennani Smires Y, Victor G, Robin G, Ribes D, Pascal P, et al. Toulouse Amyloidosis Research Network. Diagnostic score for the detection of cardiac amyloidosis in patients with left ventricular hypertrophy and impact on prognosis. *Amyloid*. Jun 2017;24(2):101-109. [doi: [10.1080/13506129.2017.1333956](https://doi.org/10.1080/13506129.2017.1333956)] [Medline: [28553897](https://pubmed.ncbi.nlm.nih.gov/28553897/)]
6. Cho H, Choi HJ, Kang HG, Ha IS, Cheong HI, Han KH, et al. Influence of the method of definition on the prevalence of left-ventricular hypertrophy in children with chronic kidney disease: data from the Know-Ped CKD study. *Kidney Blood Press Res*. 2017;42(3):406-415. [FREE Full text] [doi: [10.1159/000478867](https://doi.org/10.1159/000478867)] [Medline: [28689198](https://pubmed.ncbi.nlm.nih.gov/28689198/)]
7. Viana Gonçalves IC, Cerdeira CD, Poletti Camara E, Dias Garcia JA, Ribeiro Pereira Lima Brigagão M, Bessa Veloso Silva R, et al. Tempol improves lipid profile and prevents left ventricular hypertrophy in LDL receptor gene knockout (LDLR<sup>-/-</sup>) mice on a high-fat diet. *Rev Port Cardiol*. Sep 2017;36(9):629-638. [FREE Full text] [doi: [10.1016/j.repc.2017.02.014](https://doi.org/10.1016/j.repc.2017.02.014)] [Medline: [28826937](https://pubmed.ncbi.nlm.nih.gov/28826937/)]
8. Kitamura M, Amano Y, Takayama M, Shibuya J, Matsuda J, Sangen H, et al. Usefulness of non-anteroseptal region left ventricular hypertrophy using cardiac magnetic resonance to predict repeat alcohol septal ablation for refractory obstructive

- hypertrophic cardiomyopathy. *Am J Cardiol.* Jul 01, 2017;120(1):124-130. [doi: [10.1016/j.amjcard.2017.03.248](https://doi.org/10.1016/j.amjcard.2017.03.248)] [Medline: [28483204](https://pubmed.ncbi.nlm.nih.gov/28483204/)]
9. Tian JP, Wang J, Tian XK, Du FH, Wang T. The impact of visit-to-visit systolic blood pressure variability on residual renal function and left ventricular hypertrophy in peritoneal dialysis patients. *Turk J Med Sci.* Apr 30, 2018;48(2):279-285. [doi: [10.3906/sag-1704-92](https://doi.org/10.3906/sag-1704-92)] [Medline: [29714440](https://pubmed.ncbi.nlm.nih.gov/29714440/)]
  10. Conn NK, Schwarz KQ, Borkholder DA. In-Home cardiovascular monitoring system for heart failure: comparative study. *JMIR mHealth uHealth.* Jan 18, 2019;7(1):e12419. [FREE Full text] [doi: [10.2196/12419](https://doi.org/10.2196/12419)] [Medline: [30664492](https://pubmed.ncbi.nlm.nih.gov/30664492/)]
  11. Wang J, Tan WJ, Li X, Zhang GP, Huang JY, Chen XH, et al. [High-frequency echocardiography for assessment of regional wall motion abnormality and cardiac function in mice with myocardial infarction]. *Nan Fang Yi Ke Da Xue Xue Bao.* Aug 20, 2017;37(8):1014-1021. [FREE Full text] [Medline: [28801279](https://pubmed.ncbi.nlm.nih.gov/28801279/)]
  12. Takahashi M, Kinugawa S, Takada S, Kakutani N, Furihata T, Sobirin MA, et al. The disruption of invariant natural killer T cells exacerbates cardiac hypertrophy and failure caused by pressure overload in mice. *Exp Physiol.* Mar 18, 2020;105(3):489-501. [doi: [10.1113/EP087652](https://doi.org/10.1113/EP087652)] [Medline: [31957919](https://pubmed.ncbi.nlm.nih.gov/31957919/)]
  13. Eckert M, Volmerg JS, Friedrich CM. Augmented reality in medicine: systematic and bibliographic review. *JMIR mHealth uHealth.* Apr 26, 2019;7(4):e10967. [FREE Full text] [doi: [10.2196/10967](https://doi.org/10.2196/10967)] [Medline: [31025950](https://pubmed.ncbi.nlm.nih.gov/31025950/)]
  14. Liu L, Duan S, Zhang Y, Wu Y, Zhang L. Initial experience of the synchronized, real-time, interactive, remote transthoracic echocardiogram consultation system in rural China: longitudinal observational study. *JMIR Med Inform.* Jul 08, 2019;7(3):e14248. [FREE Full text] [doi: [10.2196/14248](https://doi.org/10.2196/14248)] [Medline: [31287062](https://pubmed.ncbi.nlm.nih.gov/31287062/)]
  15. Hendrikx G, Bauwens M, Wierts R, Mottaghy F, Post M. Left ventricular function measurements in a mouse myocardial infarction model. *Nuklearmedizin.* Mar 06, 2018;55(03):115-122. [doi: [10.3413/nukmed-0776-15-11](https://doi.org/10.3413/nukmed-0776-15-11)]

## Abbreviations

- IVS:** interventricular septal  
**LVDP:** left ventricular diastolic pressure  
**LVEDD:** left ventricular end-diastolic diameter  
**LVESD:** left ventricular end-systolic diameter  
**LVPW:** left ventricular posterior wall  
**LVSP:** left ventricular systolic pressure  
**+dp/dt max:** maximal rate of the increase of left ventricular pressure  
**-dp/dt max:** maximal rate of the decrease of left ventricular pressure

*Edited by K Kalemaki, Z Du, H Li; submitted 03.Apr.2020; peer-reviewed by Z Liu, Y Zeng, X Yang; comments to author 17.Apr.2020; revised version received 30.Apr.2020; accepted 01.May.2020; published 16.Sep.2020*

*Please cite as:*

*Chen Y, Du J, Sun X, Li Q, Qin M, Xiao Q, Bryan M*

*Retracted: Treatment of Left Ventricular Circulation Disorder: Application of Echocardiography Information Data Monitoring*  
*JMIR Med Inform 2020;8(9):e19110*

*URL: <http://medinform.jmir.org/2020/9/e19110/>*

*doi: [10.2196/19110](https://doi.org/10.2196/19110)*

*PMID: [32936076](https://pubmed.ncbi.nlm.nih.gov/32936076/)*

©Yulong Chen, Jianxia Du, Xiao Sun, Qiancheng Li, Ming Qin, Qian Xiao, Mark Bryan. Originally published in JMIR Medical Informatics (<http://medinform.jmir.org>), 16.Sep.2020. This is an open-access article distributed under the terms of the Creative Commons Attribution License (<https://creativecommons.org/licenses/by/4.0/>), which permits unrestricted use, distribution, and reproduction in any medium, provided the original work, first published in JMIR Medical Informatics, is properly cited. The complete bibliographic information, a link to the original publication on <http://medinform.jmir.org/>, as well as this copyright and license information must be included.